Antimicrobial Agents and Chemotherapy

Rilpivirine Inhibits Drug Transporters ABCB1, SLC22A1, and SLC22A2 *In Vitro*

Darren M. Moss, Neill J. Liptrott, Paul Curley, Marco Siccardi, David J. Back and Andrew Owen

Antimicrob. Agents Chemother. **2013, 57(11):5612. DOI: 10.1128/AAC.01421-13.**
Published Ahead of Print 3 September 2013.

AAC Journals.ASM.org

Rilpivirine Inhibits Drug Transporters ABCB1, SLC22A1, and SLC22A2 *In Vitro*

Darren M. Moss, Neill J. Liptrott, Paul Curley, Marco Siccardi, David J. Back, Andrew Owen

Department of Molecular and Clinical Pharmacology, University of Liverpool, Liverpool, United Kingdom

Rilpivirine is a nonnucleoside reverse transcriptase inhibitor approved for treatment of HIV-1 infection in antiretroviral-naive adult patients. Potential interactions with drug transporters have not been fully investigated. Transport by and inhibition of drug transporters by rilpivirine were analyzed to further understand the mechanisms governing rilpivirine exposure and determine the potential for transporter-mediated drug-drug interactions. The ability of rilpivirine to inhibit or be transported by ABCB1 was determined using ABCB1-overexpressing CEM_{VBL100} cells and Caco-2 cell monolayers. The *Xenopus laevis* oocyte heterologous protein expression system was used to clarify if rilpivirine was either transported by or inhibited the function of influx transporters SLCO1A2, SLCO1B1, SLCO1B3, SLC22A2, SLC22A6, and SLC22A8. The ability of rilpivirine to inhibit or be transported by SLC22A1 was determined using SLC22A1-expressing KCL22 cells. Rilpivirine showed higher accumulation in SLC22A1-overexpressing KCL22 cells than control cells (27% increase, $P = 0.03$) and inhibited the functionality of SLC22A1 and SLC22A2 transport with 50% inhibitory concentrations (IC_{50}s) of 28.5 μM and 5.13 μM, respectively. Inhibition of ABCB1-mediated digoxin transport was determined for rilpivirine, which inhibited digoxin transport in the B-to-A direction with an IC_{50} of 4.48 μM. The maximum rilpivirine concentration in plasma in patients following a standard 25-mg dosing regimen is around 0.43 μM, lower than that necessary to substantially inhibit ABCB1, SLC22A1, or SLC22A2 *in vitro*. However, these data indicate that SLC22A1 may contribute to variability in rilpivirine exposure and that interactions of rilpivirine with substrates of SLC22A1, SLC22A2, or ABCB1 may be possible.

Rilpivirine is a nonnucleoside reverse transcriptase inhibitor which has been approved for use in treatment-naive adult HIV-infected patients. The drug shows high potency, with an *in vitro* 50% effective concentration of 0.73 nM against HIV, and is associated with fewer neuropsychiatric side effects than efavirenz (1, 2).

The absorption of rilpivirine is affected by gastric pH. Omeprazole and famotidine reduced the rilpivirine maximum concentration (C_{max}) by 40% and 85%, respectively, although intake of famotidine 12 h prior to rilpivirine did not affect rilpivirine absorption (3). Food also influences rilpivirine absorption, with an ~40% increase in drug exposure seen when rilpivirine is taken with a normal or high-calorie meal compared with that seen under fasted conditions. Rilpivirine is metabolized primarily by cytochrome P450 3A (CYP3A), and drugs which inhibit or induce CYP3A may alter rilpivirine exposure in patients (4). Rilpivirine inhibits CYP3A4, CYP2B6, and CYP2C19 *in vitro*, although the ability of the drug to inhibit these enzymes *in vivo* is not fully known (5).

A recent phase III, randomized trial in treatment-naive HIV-1-infected adults (ECHO) demonstrated that rilpivirine was noninferior (efficacy) to efavirenz and had an improved safety profile compared with that of efavirenz (2). However, rilpivirine did show a higher virological failure rate than efavirenz (13% versus 6%), which was also observed in a parallel phase III trial (THRIVE) (6). The causes of this higher incidence of the virological failure rate are not fully understood, although the possibility of inadequate penetration of drug into tissues or infected cells may be a factor. Drug transporter proteins are involved in the movement of many drugs between blood and tissues and may be a factor in the disposition of several antiretrovirals (7), and an increased understanding of the role of transporters in rilpivirine disposition may help explain the observed virological failure.

The impact of drug transporters on rilpivirine disposition has not been fully investigated. In a previous study, growth inhibition assays in MDCKII cells overexpressing human ABCB1, ABCG2, ABCC1, and ABCC2 were used as a surrogate for the substrate characteristics of rilpivirine, although direct concentration measurements of rilpivirine or control substrates were not determined (5). An increased knowledge of the mechanisms that control the rilpivirine disposition may help rationalize or even anticipate drug-drug interactions (2, 6) and will identify candidate transporter genes for future pharmacogenetic studies. Of particular note, rilpivirine is known to increase the serum levels of creatinine, suggesting the possible inhibition of kidney-expressed cation transporters (2, 8). The aim of this study was to investigate the transport of rilpivirine by the efflux transporter ABCB1 (P glycoprotein) at both physiological and superphysiological levels and to investigate the potential transport of rilpivirine by major human drug influx transporters (7). Influx transporters characterized were the liver-expressed SLCO1B1 (OATPC), SLCO1B3 (OATP8), and SLC22A1 (OCT1), the kidney-expressed SLC22A2 (OCT2), SLC22A6 (OAT1), and SLC22A8 (OAT3), and the brain-expressed SLCO1A2 (OATPA) (9). Inhibition of ABCB1 and influx transporters by rilpivirine was also determined. All transporters tested, apart from SLCO1A2 and SLCO1B3, have been associated with clinical drug-drug interactions, and transporters

Received 4 July 2013 Returned for modification 13 August 2013
Accepted 24 August 2013
Published ahead of print 3 September 2013
Address correspondence to Darren M. Moss, darren.moss@liverpool.ac.uk.

doi:10.1128/AAC.01421-13

were selected using FDA and International Transporter Consortium guidelines (10, 11).

MATERIALS AND METHODS

Materials. CEM and CEM_{VBL100} cells were donated by Ross Davey, Bill Walsh Cancer Research Laboratories (St. Leonards, Australia). Caco-2 cells were purchased from the European Collection of Cell Cultures (Salisbury, United Kingdom). SLC22A1-overexpressing KCL22 cells and mock-transfected KCL22 cells were donated by Athina Giannoudis, Department of Hematology, Royal Liverpool University Hospital (Liverpool, United Kingdom). [^{14}C]rilpivirine (specific activity = 20.00 mCi/mmol) and nonradiolabeled rilpivirine were gifts from Tibotec (Mechelen, Belgium). [^{3}H]estrone-3-sulfate (specific activity = 50 Ci/mmol), [^{14}C]tetraethyl ammonium (specific activity = 55 mCi/mmol), [^{3}H]aminohippuric acid (specific activity = 5 Ci/mmol), and [^{14}C]mannitol (specific activity = 55 mCi/mmol) were purchased from American Radiolabeled Chemicals (MO). [^{3}H]digoxin (specific activity = 50 Ci/mmol) and [^{14}C]metformin (specific activity = 0.1 Ci/mmol) were purchased from PerkinElmer (Boston, MA). [^{3}H]lopinavir (specific activity = 5 Ci/mmol) was purchased from Moravek Biochemicals (CA). Lopinavir was a gift from Abbott (IL). Tariquidar (XR9576) was purchased from Xenova (Sloane, United Kingdom). cDNA clones were purchased from Source BioScience United Kingdom (Nottingham, United Kingdom). mMessage transcription kits were purchased from Ambion Ltd. (Huntingdon, United Kingdom). Ultima Gold scintillation fluid was purchased from PerkinElmer (Boston, MA). Restriction enzymes were purchased from New England BioLabs (Hitchen, United Kingdom). Adult female *Xenopus laevis* frogs were purchased from Xenopus Express (Lyon, France). All other drugs and reagents were obtained from Sigma (Poole, United Kingdom).

Accumulation experiments using CEM and CEM_{VBL100} cells. CEM and CEM_{VBL100} cells were maintained in cell culture medium (RPMI, 10% [vol/vol] fetal calf serum [FCS]) prior to the experiment (37°C, 5% CO_2). CEM cells are a wild-type T-lymphoblastoid cell line. CEM_{VBL100} cells are CEM cells which have greatly increased ABCB1 expression (selected using vinblastine up to a concentration of 100 ng/ml). On the day of the experiment, CEM and CEM_{VBL100} cells of a constant cell density (1 ml, 5×10^6 cells/ml) were incubated (37°C, 5% CO_2) for 30 min in cell culture medium (RPMI, 10% [vol/vol] FCS) containing either rilpivirine (20 μM) or a control ABCB1 substrate, lopinavir (1 μM). A separate incubation was undertaken where CEM_{VBL100} cells were preincubated prior to the substrate addition in cell culture medium containing the potent noncompetitive ABCB1 inhibitor tariquidar (RPMI, 10% [vol/vol] FCS, 300 nM tariquidar, 30 min). Tariquidar was also included during the 30-min substrate incubation. Following incubation, cells were centrifuged (800 × *g*, 1°C, 1 min) and supernatant fractions were taken for analysis. Cells were washed three times using ice-cold Hanks balanced salt solution (HBSS), centrifuged (800 × *g*, 1°C, 1 min), and lysed with the addition of 100 μl tap water. Cells were vortexed for 5 min, and samples were added to scintillation vials. Four milliliters of scintillation fluid was added to the scintillation vials, which were then loaded into a liquid scintillation analyzer (Beckman Tri-Carb). Intracellular drug concentrations were determined, assuming a volume of 1 pl per cell (12).

Bidirectional transport experiments using Caco-2 cell monolayers. Caco-2 cells were maintained in cell culture (37°C, 5% CO_2) by passaging at 70% confluence using cell culture medium (Dulbecco's modified Eagle medium [DMEM], 15% [vol/vol] FCS). The passage number of the cells used in this study was between 25 and 30. Caco-2 cell monolayers were cultured, and transwell monolayers were created as previously described (13). Briefly, confluent Caco-2 cells were seeded onto polycarbonate membrane transwells at a density of 5×10^5 cells/cm^2. Medium was initially replaced after 24 h and was then replaced every 48 h. Plates were used in the experiments at 21 days after seeding. Monolayer integrity was checked on the day of the experiment using a Millicell ERS system (Millipore) to determine the transepithelial electrical resistance (TEER) across the monolayer. A TEER of >600 Ω was deemed acceptable. In addition, radiolabeled [^{14}C]mannitol was added to each well to confirm monolayer integrity. Mannitol samples were analyzed by liquid scintillation counting (Beckman Tri-Carb), and wells were used for experimental analysis only if the apparent permeation of mannitol was less than $1 \text{ cm} \times 10^{-6} \text{ s}^{-1}$.

The movement of rilpivirine across Caco-2 cell monolayers and the impact of an ABCB1 inhibitor on this movement were assessed. The monolayer TEER was determined, the medium in each well was replaced with warm transport buffer (HBSS, 25 mM HEPES, 0.1% [wt/vol] bovine serum albumin, pH 7), and the cells and buffer were allowed to equilibrate (37°C, 30 min). For inhibition studies, this transport buffer contained tariquidar (300 nM). The transport buffer in the apical (for transport in the A-to-B direction) and basolateral (for transport in the B-to-A direction) chambers was replaced with transport buffer containing rilpivirine (20 μM) with or without 300 nM tariquidar. Samples (50 μl) were taken from the receiver compartment at 0, 30, and 60 min and replaced with an equal volume of transport buffer. Samples were analyzed using a liquid scintillation counter (Beckman Tri-Carb). Data were used to determine the rilpivirine apparent permeation (P_{app}; cm s^{-1}) for each direction and the efflux ratio (ratio of the P_{app} in the B-to-A direction to the P_{app} in the A-to-B direction). P_{app} was calculated using the following equation, as described previously: $P_{app}\,(10^{-6}) = [(dQ/dt) \times V]/(A \times C_0)$, where dQ/dt is the change in drug concentration in the receiver chamber over time (nM s^{-1}), V is the volume in the receiver compartment (ml), A is the total surface area of the transwell membrane (cm^2), C_0 is the initial drug concentration in the donor compartment (nM), and P_{app} is the apparent permeation (10^{-6} cm s^{-1}) (14).

In addition, the above-described experiment was repeated using digoxin (1 μM) as a control ABCB1 substrate and assessing the impact of rilpivirine (1, 3, 10, and 30 μM) and tariquidar (300 nM) on the digoxin P_{app} in both directions.

Production of uptake transporter cRNA for *Xenopus laevis* oocyte injection. SLCO1A2, SLCO1B1, and SLCO1B3 were cloned from cDNA extracted from Huh-7D12 and A549 cells as described previously (15). IMAGE clones of SLC22A2, SLC22A6, and SLC22A8 were purchased from Source Bioscience United Kingdom (Nottingham, United Kingdom). Transporter gene-containing plasmids from clones were extracted, linearized, and used as a template in cRNA production using a mMessage mMachine RNA transcription kit (Ambion) following the manufacturer's protocol.

***Xenopus laevis* oocyte isolation, collagenase treatment, and microinjection.** Oocytes were harvested from sacrificed adult female *Xenopus laevis* frogs and treated with modified Barth's solution not containing calcium (88 mM NaCl, 1 mM KCl, 15 mM HEPES, 100 U penicillin, 100 μg streptomycin, pH 7.4) but containing collagenase (1 mg/ml, 22°C, 60 rpm, 1 h). Cells were transferred to Barth's solution containing calcium (88 mM NaCl, 1 mM KCl, 15 mM HEPES, 0.3 mM $CaCNO_3 \cdot 6H_2O$, 41 μM $CaCl_2 \cdot 6H_2O$, 0.82 mM $MgSO_4 \cdot 7H_2O$, 100 U penicillin, 100 μg streptomycin, pH 7.4) and stored in a cold room at 8°C. Healthy cells were selected and injected with transporter cRNA (50 ng per oocyte, 1 ng/nl) or sterile water (50 nl) and maintained in Barth's solution containing calcium to allow transporter expression (5 days for SLCO1B3-injected oocytes, 3 days for all other conditions, 18°C). Barth's solution was replaced daily, and damaged oocytes were removed.

Drug accumulation in transporter RNA-injected *Xenopus laevis* oocytes. Drug accumulation studies using *X. laevis* oocytes were performed as described previously with slight modifications (15). For experiments determining rilpivirine transport, radiolabeled rilpivirine was incubated in Hanks balanced salt solution (pH 7.4) with at least 6 oocytes per condition in a 48-well Nunc flat-bottom plate (500 μl, 20 μM, room temperature, shaking at 60 rpm, 1 h). Radiolabeled positive-control drugs were tested alongside rilpivirine to confirm successful transporter expression. The positive-control drugs used were estrone-3-sulfate (1 μM) for SLCO1A2, SLCO1B1, and SLCO1B3, aminohippuric acid (1 μM) for SLC22A6, and metformin (2 μM) for SLC22A2. Inhibition of drug trans-

porters by rilpivirine was initially assessed by coincubating positive-control substrates with 10 μM rilpivirine. SLC22A2-mediated metformin transport was reduced in the presence of rilpivirine; therefore, a 50% inhibitory concentration (IC_{50}) curve was determined using 1, 2.5, 5, 10, 25, 50, and 100 μM rilpivirine. All incubations were terminated by transferring oocytes to cell strainers and washing in ice-cold HBSS to remove extracellular drug. Each oocyte was placed in a separate scintillation vial, followed by addition of 100 μl 10% SDS. After disintegration of the oocytes by the SDS, 4 ml scintillation fluid was added to all vials, which were then loaded into a liquid scintillation analyzer (Beckman Tri-Carb). Results are expressed as the concentration (μM) of drug in oocytes ± standard deviation (SD), assuming that each oocyte had a volume of 1 μl (15).

Creation and culture of mock-transfected and SLC22A1-expressing KCL22 cells. KCL22 cells were maintained in cell culture medium (RPMI, 10% [vol/vol] FCS) prior to the experiment in a CO_2 incubator (37°C, 5% CO_2). SLC22A1-expressing KCL22 cells and mock-transfected KCL22 cells were created previously by Athina Giannoudis at the Department of Hematology, Royal Liverpool University Hospital, Liverpool, United Kingdom (16). In the previous work, SLC22A1-overexpressing KCL22 cells were created by transfecting plasmid pcDNA-hSLC22A1 into cells by nucleofection. Similarly, mock-transfected KCL22 cells were created by transfecting the empty vector pcDNA3.1 into cells by nucleofection. Transfected cells were selected using neomycin, and stable cell lines were established. KCL22 cells were used for human SLC22A1 transfection because it expresses a small basal amount of SLC22A1 in comparison to other chronic myelogenous leukemia cell lines (17).

Rilpivirine accumulation and inhibitory potential in SLC22A1-overexpressing KCL22 cells. On the day of the experiment, mock-transfected KCL22 cells and SLC22A1-expressing KCL22 cells of a constant cell density (1 ml, 2.5×10^6 cells/ml) were incubated (37°C, 5% CO_2) for 30 min in cell culture medium (RPMI, 10% [vol/vol] FCS) containing either rilpivirine (20 μM) or the control SLC22A1 substrate tetraethyl ammonium (1 μM). A separate incubation was undertaken, where SLC22A1-expressing KCL22 cells were preincubated prior to the substrate addition in cell culture medium containing the potent SLC22A1 inhibitor prazosin (RPMI, 10% [vol/vol] FCS, 100 μM prazosin, 30 min). Prazosin was also included during the 30-min substrate incubation. Following incubation, cells were centrifuged (800 × *g*, 1°C, 1 min) and processed for analysis as described for CEM cells. Using intracellular radioactivity readings, cellular drug concentrations (μM) ± SD were determined in each cell line, assuming a 1-pl volume per cell.

The inhibitory potential of rilpivirine for SLC22A1 transport was assessed. Accumulation of tetraethyl ammonium (5.5 μM) was determined when cells were coincubated with a log range of rilpivirine concentrations (0, 1, 2.5, 5, 10, 25, 50, 100 μM). A parallel experiment was performed using prazosin as a positive-control SLC22A1 inhibitor. Data were plotted using Prism (version 5) software, and slopes were used to calculate the relative IC_{50} (the amount of drug needed to achieve 50% SLC22A1 inhibition, as determined from the maximum and minimum extremes of the nonlinear regression plot).

Statistical analysis. Data were analyzed using SPSS (version 19) for Windows. IC_{50} curves were generated using Prism (version 5) for Windows. All data were tested for normality using the Shapiro-Wilk test. An independent *t* test was used to determine the significance of normally distributed data, and the Mann-Whitney U test was used for all other data. A two-tailed *P* value of <0.05 was accepted as being statistically significant.

RESULTS

Rilpivirine accumulation in wild-type and ABCB1-overexpressing CEM cells. Cellular accumulation of rilpivirine was determined in CEM and ABCB1-overexpressing CEM_{VBL100} cells, and the effect of the ABCB1 inhibitor tariquidar on this accumulation was investigated (Fig. 1A). Rilpivirine accumulation in CEM_{VBL100} cells (54.1 ± 1.6 μM) was not significantly different from that in CEM cells (48.7 ± 1.9 μM, $P = 0.11$). Tariquidar treatment did not alter rilpivirine accumulation in CEM_{VBL100} cells ($P = 0.23$). The control ABCB1 substrate lopinavir had lower accumulation in CEM_{VBL100} cells (10.3 ± 0.9 μM) than in CEM cells (17.9 ± 1.5 μM, $P < 0.01$) (Fig. 1B). This difference in lopinavir accumulation between CEM and CEM_{VBL100} cells was lost when CEM_{VBL100} cells were treated with tariquidar (19.8 ± 0.7 μM, $P = 0.10$).

Impact of tariquidar on rilpivirine Caco-2 cell monolayer permeation. The P_{app} values obtained for rilpivirine with and without tariquidar are given in Fig. 1C. All P_{app} values and efflux ratio calculations were made using the samples taken after 60 min of incubation as sink conditions were maintained. Rilpivirine showed significantly higher transport in the B-to-A direction ($P_{app} = 6.6 \times 10^{-6} \pm 0.6 \times 10^{-6}$ cm s^{-1}) than in the A-to-B direction ($P_{app} = 4.0 \times 10^{-6} \pm 0.7 \times 10^{-6}$ cm s^{-1}, $P < 0.01$). The efflux ratio (P_{app} in the B-to-A direction/P_{app} in the A-to-B direction) of rilpivirine at 60 min was 1.65. When incubations were repeated in the presence of the ABCB1 inhibitor tariquidar, no significant alteration in rilpivirine permeation was determined in either the A-to-B direction ($P_{app} = 3.9 \times 10^{-6} \pm 0.7 \times 10^{-6}$ cm s^{-1}, $P = 0.88$) or the B-to-A direction ($P_{app} = 6.6 \times 10^{-6} \pm 0.9 \times 10^{-6}$ cm s^{-1}, $P = 0.93$).

Impact of rilpivirine on digoxin Caco-2 cell monolayer permeation. The ability of rilpivirine to inhibit ABCB1-mediated transport of digoxin was assessed using Caco-2 cell monolayers (Fig. 1D). Permeation of 1 μM digoxin in the A-to-B direction was significantly increased when it was coincubated with rilpivirine at 1 μM ($P_{app} = 2.1 \times 10^{-6} \pm 0.3 \times 10^{-6}$ cm s^{-1}, $P = 0.01$), 3 μM ($P_{app} = 4.2 \times 10^{-6} \pm 1.6 \times 10^{-6}$ cm s^{-1}, $P = 0.04$), 10 μM ($P_{app} = 10.9 \times 10^{-6} \pm 2.5 \times 10^{-6}$ cm s^{-1}, $P < 0.01$), and 30 μM ($P_{app} = 12.1 \times 10^{-6} \pm 0.2 \times 10^{-6}$ cm s^{-1}, $P < 0.01$) compared with that for the rilpivirine-free controls ($P_{app} = 1.3 \times 10^{-6} \pm 0.1 \times 10^{-6}$ cm s^{-1}). Permeation of 1 μM digoxin in the B-to-A direction was significantly decreased when it was coincubated with 10 μM rilpivirine [$P_{app} = (22.2 \pm 6.0) \times 10^{-6}$ cm s^{-1}, $P = 0.02$] and 30 μM rilpivirine [$P_{app} = (18.2 \pm 2.7) \times 10^{-6}$ cm s^{-1}, $P = 0.01$], compared with rilpivirine-free control incubations [$P_{app} = (64.2 \pm 8.6) \times 10^{-6}$ cm s^{-1}]. Rilpivirine reduced permeation in the A-to-B direction, permeation in the B-to-A direction, and the efflux ratio of digoxin with IC_{50}s of 4.24 μM (95% confidence interval [CI], 2.94 to 6.10 μM), 4.48 μM (95% CI, 2.52 to 7.96 μM), and 1.08 μM (95% CI, 0.67 to 1.73 μM), respectively. The control ABCB1 inhibitor tariquidar increased the permeation of digoxin in the A-to-B direction ($P_{app} = 16.6 \times 10^{-6} \pm 3.4 \times 10^{-6}$ cm s^{-1}, $P = 0.02$) and decreased the permeation of digoxin in the B-to-A direction ($P_{app} = 14.7 \times 10^{-6} \pm 3.6 \times 10^{-6}$ cm s^{-1}, $P < 0.01$), resulting in a digoxin efflux ratio of 0.9 (Fig. 1D).

Rilpivirine accumulation and inhibitory potential in transporter cRNA-injected *Xenopus laevis* oocytes. The accumulation of rilpivirine was determined in SLCO1A2, SLCO1B1, SLCO1B3, SLC22A2, SLC22A6, and SLC22A8 cRNA-injected *X. laevis* oocytes. Water-injected oocytes were also used in accumulation experiments to determine passive diffusion of the drug into oocytes, and control substrates were used to validate functional transporter expression. The control substrates used were estrone-3-sulfate (SLC22A8, SLCO1A2, SLCO1B1, SLCO1B3), aminohippuric acid (SLC22A6), and metformin (SLC22A2). The ability of rilpivirine to inhibit accumulation of control substrates was also assessed. The amount of drug accumulation in transporter cRNA-injected oocytes compared to that in water-injected control oocytes was determined and is given in Fig. 2.

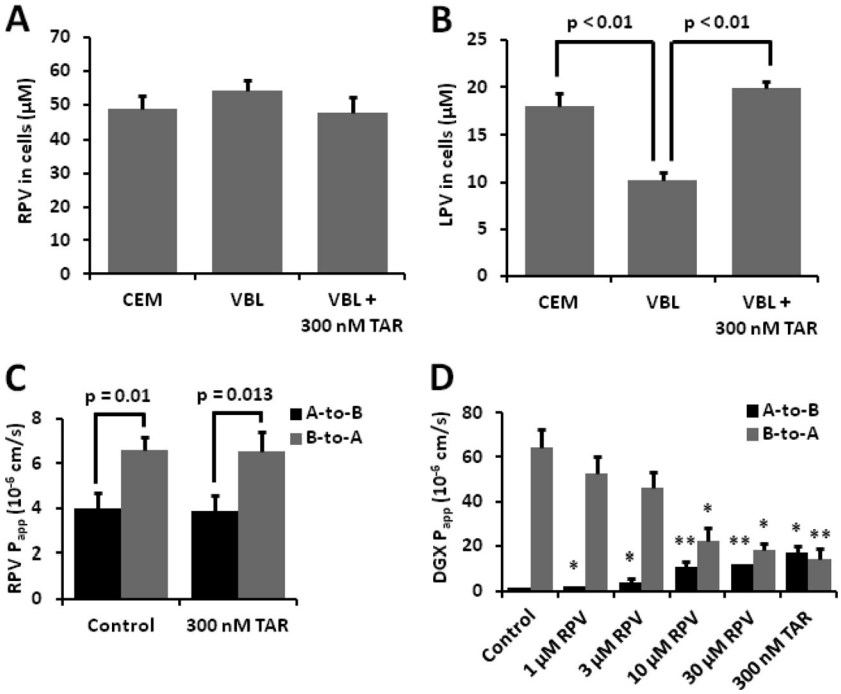

FIG 1 (A) Rilpivirine (RPV) accumulation in CEM, CEM_{VBL100} (VBL), and CEM_{VBL100} cells treated with 300 nM tariquidar. Data are expressed as mean the rilpivirine concentration in cells (μM; $n = 3$ experimental replicates) ± SD. (B) Lopinavir (LPV) accumulation in CEM, CEM_{VBL100}, and CEM_{VBL100} cells treated with 300 nM tariquidar (TAR). Data are expressed as the mean lopinavir concentration in cells (μM; $n = 3$ experimental replicates) ± SD. (C) Permeation of rilpivirine in the A-to-B (black bars) and B-to-A (gray bars) directions across a Caco-2 cell monolayer with and without the presence of 300 nM tariquidar. Data are expressed as the mean P_{app} (10^{-6} cm s^{-1}; $n = 3$ experimental replicates) ± SD. (D) Permeation of digoxin (DGX) in the A-to-B (black bars) and B-to-A (gray bars) directions across a Caco-2 cell monolayer with and without the presence of a range of rilpivirine concentrations or 300 nM tariquidar. Data are expressed as the mean P_{app} (10^{-6} cm^{-1}; $n = 3$ experimental replicates) ± SD. *, $P < 0.05$; **, $P = 0.01$.

Rilpivirine accumulation was not altered in oocytes expressing SLC22A2 (68.55 ± 12.22 μM, $P = 0.14$), SLC22A6 (54.80 ± 5.44 μM, $P = 0.09$), SLC22A8 (62.67 ± 5.91 μM, $P = 0.72$), SLCO1A2 (66.50 ± 6.93 μM, $P = 0.65$), SLCO1B1 (67.72 ± 15.16 μM, $P = 0.38$), or SLCO1B3 (73.27 ± 10.03 μM, $P = 0.41$) in comparison to that in water-injected control oocytes (60.31 ± 2.81 μM) (Fig. 2A). Estrone-3-sulfate accumulation was higher in oocytes expressing SLC22A8 (0.62 ± 0.10 μM, $P = 0.002$), SLCO1A2 (3.63 ± 0.52 μM, $P < 0.001$), SLCO1B1 (5.95 ± 0.62 μM, $P < 0.001$), and SLCO1B3 (0.45 ± 0.04 μM, $P = 0.009$) than in water-injected control oocytes (0.24 ± 0.05 μM). Aminohippuric acid accumulation was higher in oocytes expressing SLC22A6 (6.07 ± 0.54 μM, $P = 0.002$) than in water-injected control oocytes (0.22 ± 0.01 μM). Metformin accumulation was higher in oocytes expressing SLC22A2 (1.36 ± 0.16 μM, $P < 0.001$) than in water-injected control oocytes (0.23 ± 0.06 μM). Rilpivirine at 10 μM did not alter the accumulation of estrone-3-sulfate in oocytes expressing SLC22A8 ($P = 0.92$), SLCO1A2 ($P = 0.83$), SLCO1B1 ($P = 0.38$), or SLCO1B3 ($P = 0.53$) (Fig. 2B) and also did not alter the accumulation of aminohippuric acid in oocytes expressing SLC22A6 ($P = 0.64$) (Fig. 2C). Accumulation of metformin in oocytes expressing SLC22A2 was reduced in the presence of rilpivirine; therefore, the IC_{50}s determined for rilpivirine and the control SLC22A2 inhibitor quinidine were 5.13 μM and 40.45 μM, respectively (Fig. 2D).

Rilpivirine accumulation and inhibitory potential in SLC22A1-expressing KCL22 cells. The accumulation of rilpivirine in transfected SLC22A1-expressing KCL22 cells and mock-transfected KCL22 cells was determined and compared to the rilpivirine accumulation in cells coincubated with the SLC22A1 inhibitor prazosin. Accumulation of the control SLC22A1 substrate tetraethyl ammonium was also determined.

Rilpivirine showed a small but statistically significantly higher accumulation in SLC22A1-expressing KCL22 cells (88.8 ± 5.9 μM, $P = 0.031$) than in mock-transfected cells (70.0 ± 8.0 μM) (Fig. 3B). The control inhibitor prazosin caused a small but significant decrease in rilpivirine cellular accumulation in SLC22A1-expressing cells (14% reduction, $P = 0.04$). Tetraethyl ammonium showed higher accumulation in SLC22A1-expressing KCL22 cells (1.6 ± 0.02 μM, $P < 0.01$) than in mock-transfected cells (0.12 ± 0.01 μM) (Fig. 3A). Prazosin decreased tetraethyl ammonium cellular accumulation in SLC22A1-expressing cells (77% reduction, $P < 0.01$). The inhibition of SLC22A1 was determined using a concentration range of rilpivirine and prazosin and used to calculate IC_{50}s (Fig. 3C). Rilpivirine inhibited tetraethyl ammonium accumulation in SLC22A1-overexpressing cells with a relative IC_{50} of 28.5 μM. Prazosin (100 μM) achieved an 84% reduction in cellular tetraethyl ammonium accumulation and a relative IC_{50} of 2.3 μM, which are similar to data in the literature (18).

DISCUSSION

Drug interactions involving antiretroviral drugs can potentially lead to therapy failure and/or exacerbate adverse drug reactions. In this study, we have investigated the interactions of rilpivirine

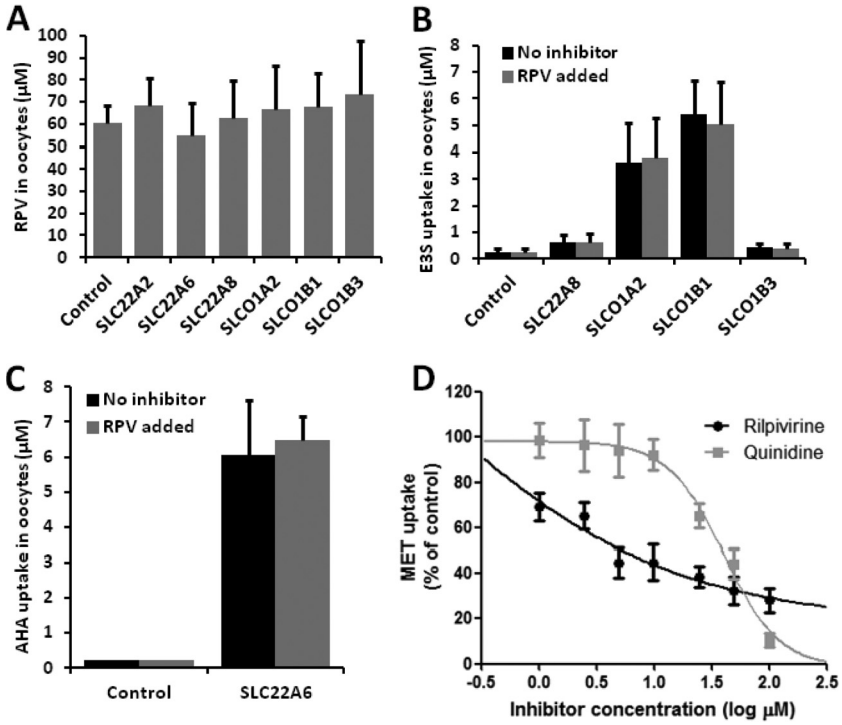

FIG 2 (A) Accumulation of rilpivirine (RPV) in *X. laevis* oocytes expressing various drug transporters (1 h, room temperature). Data are expressed as the rilpivirine oocyte concentration (μM; $n \leq 6$ experimental replicates) ± SD. (B) Accumulation of the control substrate estrone-3-sulfate (E3S) in *X. laevis* oocytes expressing various drug transporters with and without the addition of 10 μM rilpivirine. Data are expressed as the mean estrone-3-sulfate oocyte concentration (μM; $n \leq 7$ experimental replicates) ± SD. (C) Accumulation of control substrate aminohippuric acid (AHA) in *X. laevis* oocytes expressing SLC22A6 with and without the addition of 10 μM rilpivirine. Data are expressed as the mean aminohippuric acid oocyte concentration (μM; $n = 8$ experimental replicates) ± SD. (D) Inhibition of metformin (MET) accumulation in SLC22A2-expressing *X. laevis* oocytes using a concentration range of rilpivirine or the control SLC22A2 inhibitor quinidine. Data are expressed as the mean percentage of metformin accumulation compared to the level of accumulation in drug-free control oocytes ($n \leq 6$ experimental replicates) ± SE.

with a selection of key drug transporters to improve our understanding of the factors involved in rilpivirine pharmacokinetics.

The results from accumulation and bidirectional monolayer permeation experiments confirm that rilpivirine is not transported by ABCB1. The extent of rilpivirine transport by ABCB1 was not significant compared to the transport of the positive controls lopinavir and the cardiac glycoside digoxin. Indeed, the FDA guidelines recommend that a drug should achieve an efflux ratio of at least 2 in Caco-2 cell monolayers and show a greater than 50% reduction in efflux ratio when an ABCB1 inhibitor is used, in order for ABCB1 transport to be considered relevant *in vivo* (19). In our Caco-2 cell experiment, rilpivirine achieved an efflux ratio of only 1.65, with no alteration observed when tariquidar was used to inhibit ABCB1. The small efflux ratio obtained for rilpivirine suggests that active efflux in the gut is unlikely to be important *in vivo*. Therefore, no other intestinal efflux transporters were assessed in this study.

Rilpivirine inhibited ABCB1-mediated transport of digoxin through Caco-2 cell monolayers. This suggests that rilpivirine may influence the movement of ABCB1 substrates across cell membrane barriers which are high in ABCB1 expression, such as the mucosal surface epithelial cells in the intestine, the biliary canalicular surface of hepatocytes in the liver, the brush border membrane of renal proximal tubular cells in the kidney, and the blood-brain barrier (8, 20–22). However, rilpivirine did not alter the exposure of the ABCB1 substrate digoxin in healthy volunteers, which suggests that the observed *in vitro* inhibition of ABCB1 by rilpivirine is not clinically relevant (4).

In oocyte accumulation studies, rilpivirine was not a substrate of any transporter tested but did inhibit SLC22A2-mediated transport of the antidiabetic drug metformin with an IC_{50} of 5.13 μM. Therefore, there is the potential for an interaction between rilpivirine and other SLC22A2 substrates, although this will depend on the concentration of inhibitor [*I*] and the IC_{50} (i.e., [*I*]/IC_{50}). Given that the rilpivirine concentration ($C_{max} = 0.43$ μM) (3) is less than the IC_{50}, it seems unlikely that this will be a mechanism of clinically relevant interactions or would fully explain the small increase in creatinine levels in patients taking rilpivirine (8). This is in contrast to the findings for dolutegravir, as the drug causes notable inhibition of SLC22A2 *in vitro* ($IC_{50} = 1.9$ μM) at a concentration which is about 4-fold lower than the C_{max} ([*I*]/$IC_{50} = 4.2$) (23). This inhibition is consistent with the 10 to 14% increase in serum creatinine observed in patients taking dolutegravir (24). A recent publication by Weiss et al. used transfected HEK293 cells to show that rilpivirine was a weak inhibitor of SLCO1B1 and SLCO1B3 only at superphysiological concentrations (5). Furthermore, there have been no clinical interactions reported which would suggest that rilpivirine can alter the disposition of SLCO substrates; therefore, the potential for SLCO-mediated interactions is unlikely.

SLC22A1 is predominantly expressed in the liver and acts to remove substrates from the blood and into hepatic cells. The nu-

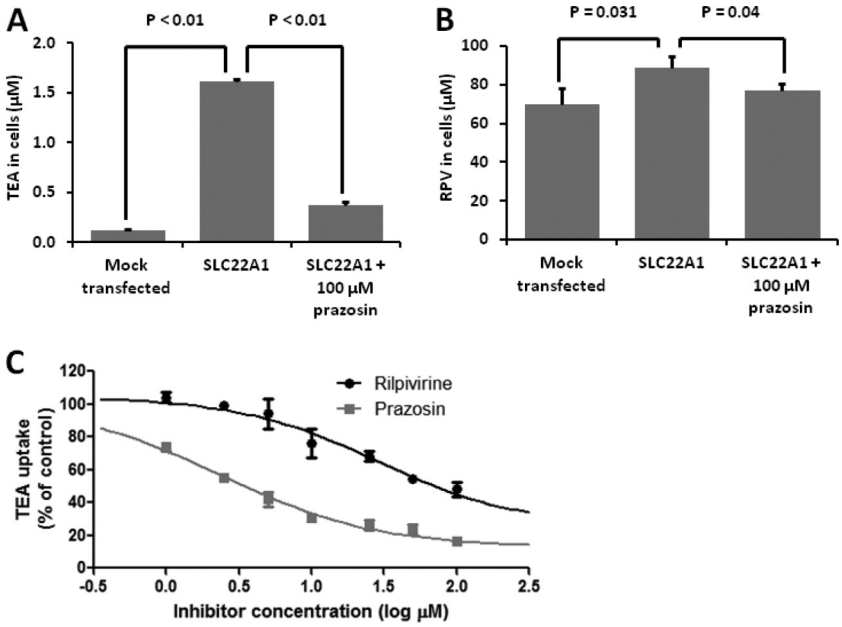

FIG 3 (A) Tetraethyl ammonium (TEA) accumulation in mock-transfected KCL22 cells, SLC22A1-expressing KCL22 cells, and SLC22A1-expressing KCL22 cells treated with 100 μM prazosin. (B) Rilpivirine (RPV) accumulation in mock-transfected KCL22 cells, SLC22A1-expressing KCL22 cells, and SLC22A1-expressing KCL22 cells treated with 100 μM prazosin. The data in panels A and B are expressed as the mean drug concentration in cells (μM; $n = 3$ experimental replicates) ± SD. (C) Inhibition of tetraethyl ammonium accumulation in SLC22A1-expressing KCL22 cells using a range of concentrations of rilpivirine or the control SLC22A1 inhibitor prazosin. Data are expressed as the mean percentage of tetraethyl ammonium accumulation compared to the level of accumulation in drug-free control cells ($n = 3$ experimental replicates) ± SD.

cleoside reverse transcriptase inhibitors (NRTIs) lamivudine and zalcitabine are substrates of SLC22A1, and several protease inhibitors inhibit SLC22A1-mediated transport of these NRTIs *in vitro* (25, 26). In the accumulation studies using transfected KCL22 cells, rilpivirine inhibited SLC22A1-mediated transport of tetraethyl ammonium, which suggests the potential for an interaction between rilpivirine and other SLC22A1 substrates. However, it should be noted that passive diffusion of rilpivirine predominated in KCL22 cells and the level of transport by SLC22A1 was low in comparison.

In summary, rilpivirine shows inhibition of ABCB1, SLC22A1, and SLC22A2 *in vitro*. However, the data should be interpreted in the context that the rilpivirine peak plasma concentration following administration of the standard 25-mg dose is approximately 0.43 μM and that plasma protein binding is 99.7% (3, 5). Nonetheless, it is not possible to rule out the possibility of the involvement of these transporters in rilpivirine-mediated drug-drug interactions because of the difficulties in extrapolating from *in vitro* data to *in vivo* phenotypes. Since different substrates have different affinities for transporters and since this interaction is likely to be competitive, the IC_{50} may be different for other drug substrates. Also, rilpivirine may concentrate in specific tissues, raising the concentrations available for transporter inhibition.

ACKNOWLEDGMENTS

This study was supported by internal funding.

David J. Back has received consultancy, honorarium, and grant income from Janssen. None of the other authors has a conflict of interest to declare.

REFERENCES

1. **Azijn H, Tirry I, Vingerhoets J, de Bethune MP, Kraus G, Boven K, Jochmans D, Van Craenenbroeck E, Picchio G, Rimsky LT.** 2010. TMC278, a next-generation nonnucleoside reverse transcriptase inhibitor (NNRTI), active against wild-type and NNRTI-resistant HIV-1. Antimicrob. Agents Chemother. **54:**718–727.
2. **Molina JM, Cahn P, Grinsztejn B, Lazzarin A, Mills A, Saag M, Supparatpinyo K, Walmsley S, Crauwels H, Rimsky LT, Vanveggel S, Boven K, ECHO Study Group.** 2011. Rilpivirine versus efavirenz with tenofovir and emtricitabine in treatment-naive adults infected with HIV-1 (ECHO): a phase 3 randomised double-blind active-controlled trial. Lancet **378:**238–246.
3. **Sharma M, Saravolatz LD.** 2013. Rilpivirine: a new non-nucleoside reverse transcriptase inhibitor. J. Antimicrob. Chemother. **68:**250–256.
4. **Crauwels H, van Heeswijk RP, Stevens M, Buelens A, Vanveggel S, Boven K, Hoetelmans R.** 2013. Clinical perspective on drug-drug interactions with the non-nucleoside reverse transcriptase inhibitor rilpivirine. AIDS Rev. **15:**87–101.
5. **Weiss J, Haefeli WE.** 2013. Potential of the novel antiretroviral drug rilpivirine to modulate the expression and function of drug transporters and drug-metabolising enzymes in vitro. Int. J. Antimicrob. Agents **41:**484–487.
6. **Cohen CJ, Andrade-Villanueva J, Clotet B, Fourie J, Johnson MA, Ruxrungtham K, Wu H, Zorrilla C, Crauwels H, Rimsky LT, Vanveggel S, Boven K, THRIVE Study Group.** 2011. Rilpivirine versus efavirenz with two background nucleoside or nucleotide reverse transcriptase inhibitors in treatment-naive adults infected with HIV-1 (THRIVE): a phase 3, randomised, non-inferiority trial. Lancet **378:**229–237.
7. **Kis O, Robillard K, Chan GN, Bendayan R.** 2010. The complexities of antiretroviral drug-drug interactions: role of ABC and SLC transporters. Trends Pharmacol. Sci. **31:**22–35.
8. **Cohen CJ, Molina JM, Cassetti I, Chetchotisakd P, Lazzarin A, Orkin C, Rhame F, Stellbrink HJ, Li T, Crauwels H, Rimsky L, Vanveggel S, Williams P, Boven K.** 2013. Week 96 efficacy and safety of rilpivirine in treatment-naive, HIV-1 patients in two phase III randomised trials. AIDS **27:**939–950.
9. **Bleasby K, Castle JC, Roberts CJ, Cheng C, Bailey WJ, Sina JF, Kulkarni AV, Hafey MJ, Evers R, Johnson JM, Ulrich RG, Slatter JG.** 2006. Expression profiles of 50 xenobiotic transporter genes in humans and pre-clinical species: a resource for investigations into drug disposition. Xenobiotica **36:**963–988.

10. **Zhang L, Reynolds KS, Zhao P, Huang SM.** 2010. Drug interactions evaluation: an integrated part of risk assessment of therapeutics. Toxicol. Appl. Pharmacol. **243:**134–145.
11. **International Transporter Consortium, Giacomini KM, Huang SM, Tweedie DJ, Benet LZ, Brouwer KL, Chu X, Dahlin A, Evers R, Fischer V, Hillgren KM, Hoffmaster KA, Ishikawa T, Keppler D, Kim RB, Lee CA, Niemi M, Polli JW, Sugiyama Y, Swaan PW, Ware JA, Wright SH, Yee SW, Zamek-Gliszczynski MJ, Zhang L.** 2010. Membrane transporters in drug development. Nat. Rev. Drug Discov. **9:**215–236.
12. **Janneh O, Chandler B, Hartkoorn R, Kwan WS, Jenkinson C, Evans S, Back DJ, Owen A, Khoo SH.** 2009. Intracellular accumulation of efavirenz and nevirapine is independent of P-glycoprotein activity in cultured CD4 T cells and primary human lymphocytes. J. Antimicrob. Chemother. **64:**1002–1007.
13. **Moss DM, Kwan WS, Liptrott NJ, Smith DL, Siccardi M, Khoo SH, Back DJ, Owen A.** 2011. Raltegravir is a substrate for SLC22A6: a putative mechanism for the interaction between raltegravir and tenofovir. Antimicrob. Agents Chemother. **55:**879–887.
14. **Elsby R, Surry DD, Smith VN, Gray AJ.** 2008. Validation and application of Caco-2 assays for the in vitro evaluation of development candidate drugs as substrates or inhibitors of P-glycoprotein to support regulatory submissions. Xenobiotica **38:**1140–1164.
15. **Hartkoorn RC, Kwan WS, Shallcross V, Chaikan A, Liptrott N, Egan D, Sora ES, James CE, Gibbons S, Bray PG, Back DJ, Khoo SH, Owen A.** 2010. HIV protease inhibitors are substrates for OATP1A2, OATP1B1 and OATP1B3 and lopinavir plasma concentrations are influenced by SLCO1B1 polymorphisms. Pharmacogenet. Genomics **20:**112–120.
16. **Giannoudis A, Davies A, Lucas CM, Harris RJ, Pirmohamed M, Clark RE.** 2008. Effective dasatinib uptake may occur without human organic cation transporter 1 (hOCT1): implications for the treatment of imatinib-resistant chronic myeloid leukemia. Blood **112:**3348–3354.
17. **Thomas J, Wang L, Clark RE, Pirmohamed M.** 2004. Active transport of imatinib into and out of cells: implications for drug resistance. Blood **104:**3739–3745.
18. **Minematsu T, Iwai M, Umehara K, Usui T, Kamimura H.** 2010. Characterization of human organic cation transporter 1 (OCT1/SLC22A1)- and OCT2 (SLC22A2)-mediated transport of 1-(2-methoxyethyl)-2-methyl-4,9-dioxo-3-(pyrazin-2-ylmethyl)-4,9-dihydro-1H-naphtho[2,3-d]imidazolium bromide (YM155 monobromide), a novel small molecule survivin suppressant. Drug Metab. Dispos. **38:**1–4.
19. **Huang SM, Strong JM, Zhang L, Reynolds KS, Nallani S, Temple R, Abraham S, Habet SA, Baweja RK, Burckart GJ, Chung S, Colangelo P, Frucht D, Green MD, Hepp P, Karnaukhova E, Ko HS, Lee JI, Marroum PJ, Norden JM, Qiu W, Rahman A, Sobel S, Stifano T, Thummel K, Wei XX, Yasuda S, Zheng JH, Zhao H, Lesko LJ.** 2008. New era in drug interaction evaluation: US Food and Drug Administration update on CYP enzymes, transporters, and the guidance process. J. Clin. Pharmacol. **48:**662–670.
20. **Lindell M, Karlsson MO, Lennernas H, Pahlman L, Lang MA.** 2003. Variable expression of CYP and Pgp genes in the human small intestine. Eur. J. Clin. Invest. **33:**493–499.
21. **Thiebaut F, Tsuruo T, Hamada H, Gottesman MM, Pastan I, Willingham MC.** 1987. Cellular localization of the multidrug-resistance gene product P-glycoprotein in normal human tissues. Proc. Natl. Acad. Sci. U. S. A. **84:**7735–7738.
22. **Ernest S, Rajaraman S, Megyesi J, Bello-Reuss EN.** 1997. Expression of MDR1 (multidrug resistance) gene and its protein in normal human kidney. Nephron **77:**284–289.
23. **Reese MJ, Savina PM, Generaux GT, Tracey H, Humphreys JE, Kanaoka E, Webster LO, Harmon KA, Clarke JD, Polli JW.** 2013. In vitro investigations into the roles of drug transporters and metabolizing enzymes in the disposition and drug interactions of dolutegravir, a HIV integrase inhibitor. Drug Metab. Dispos. **41:**353–361.
24. **van Lunzen J, Maggiolo F, Arribas JR, Rakhmanova A, Yeni P, Young B, Rockstroh JK, Almond S, Song I, Brothers C, Min S.** 2012. Once daily dolutegravir (S/GSK1349572) in combination therapy in antiretroviral-naive adults with HIV: planned interim 48 week results from SPRING-1, a dose-ranging, randomised, phase 2b trial. Lancet Infect. Dis. **12:**111–118.
25. **Jung N, Lehmann C, Rubbert A, Knispel M, Hartmann P, van Lunzen J, Stellbrink HJ, Faetkenheuer G, Taubert D.** 2008. Relevance of the organic cation transporters 1 and 2 for antiretroviral drug therapy in human immunodeficiency virus infection. Drug Metab. Dispos. **36:**1616–1623.
26. **Zhang L, Gorset W, Washington CB, Blaschke TF, Kroetz DL, Giacomini KM.** 2000. Interactions of HIV protease inhibitors with a human organic cation transporter in a mammalian expression system. Drug Metab. Dispos. **28:**329–334.